Synthesis and Process Parametric Effects on the Photocatalyst Efficiency of CuO Nanostructures for Decontamination of Toxic Heavy Metal Ions

Assefu Kassegn Sibhatu [a], Getu Kassegn Weldegebrieal [b*] , Shahla Imteyaz[c] , Suresh Sagadevan [d*], Nam Nghiep Tran[e] and Volker Hessel[e*]

[a]Department of Physics, College of Natural and Computational Sciences, Debre Berhan University, Ethiopia

[b]Department Chemistry, College of Natural and Computational Sciences, Debre Berhan University, Ethiopia

[c]CSIR-Research Associate, Department of Chemistry, Aligarh Muslim University, India

[d]Nanotechnology & Catalysis Research Centre, University of Malaya, Kuala Lumpur 50603, Malaysia

[e]School of Chemical Engineering and Advanced Materials, The University of Adelaide, North Terrace Campus, Adelaide 5005, Australia

Corresponding author e-mail: belay.kassegn@gmail.com; drsureshnano@gmail.com; volker.hessel@adelaide.edu.au

Abstract

Among the various environmental pollutants, wastewater from textile dye industries is a major concern. The textile dye industry's effluents contain complex dyes, organic and inorganic salts, acids, and heavy metals which are difficult to decompose in water as they are resistant to biodegradation. Conventional methods for dye removal are not as effective due to dyes nonbiodegradability and high solubility in water. Photocatalysis is an advanced oxidation process that is effective at degrading recalcitrant organic contaminants. It produces strong reactive oxidants like oxygen or free radical species (hydroxyl radical, and superoxide anion

radical) to degrade pollutants into nontoxic molecules Photocatalysis is proposed to be used in conjunction with other treatment processes, such as biological treatments, to reduce total organic carbon, break down macromolecular organic compounds, increase biodegradability, and to reduce the toxicity of produced water. Through oxidation or reduction reactions, toxic metal ions are converted to their metallic element state, metal oxides, or their valence to non-toxic or lower toxicity. Therefore, the present review focuses on the CuO nanostructures photocatalytic reduction of metal ions from aqueous media. The impact of synthesis (material) and their process (catalyst, radiation) parameters on the photocatalytic activity is overviewed which is the fundamental, and physical source for process intensification. Furthermore, the synthesis and process intensification processes have been discussed in detail considering their impact on elimination and toxicity of heavy metal ions.

Keywords: CuO Nanostructures, pH, catalyst dose, energy and intensity of radiation and Wastewater treatment

1.Introduction

The hazardous and toxicity of dye materials, even in low concentration, has a harmful impact on ecological systems [1-3]. It releases a large number of contaminants into the water, resulting in unusable water. Dyes inhibit photosynthesis by obstructing light transmission, resulting in low dissolved oxygen levels in water [4-6]. Fenton, activated carbon, membrane, biological and natural materials [7], algae [8], bagasse [9, 10] and plants [11] were some of the adsorbent materials that are being used by scientists for dye and heavy metal removal from waste water effluents. Despite their effectiveness, these approaches have significant drawbacks. The Fenton method, for example, necessitates a large amount of reagent, and activated carbon removes color with some contamination [12, 13]. Use of natural materials like horn snail and mud crab [14, 15] are some of the low-cost adsorbents for heavy metal removal. However, their

feasibility is with only limited to few metals. Adsorption has been the most considered method for easy, simple, flexible and low-cost operation. Rana *et. al.* [16-19] have shown various efficient membrane-based adsorption for the heavy metal ion removal. However, the low trace adsorption of heavy metals and inefficient regeneration processes lead scientist to further explore other method [20].

In this regard, degrading the dye without using reagents or producing hazardous by-products is photon-based oxidation. This method has gotten a lot of attention because of its eco-friendly technology, free energy, and renewable nature. It uses little chemical and mostly lead to no sludge production [20]. Furthermore, the use of sunlight as a source of photo deterioration increases its commercial viability [21-23]. At the moment, more than 80% of global energy consumption is derived from non-renewable fossil fuels such as coal, natural gas, and oil. During the energy production process, fossil fuels are burned, resulting in the emission of CO_2 and other harmful gases, causing climate change and environmental pollution [24]. As a result, there is a need for the advancement of energy consumption technology to include eco-friendly and renewable energy sources to aid in the transition to a low-carbon economy. A practical way to use renewable and clean energy sources is to store energy when it is abundant and use it when it is needed [25]. As per all those benefits, photon-based oxidation processing has advantages in terms of environmental friendliness, ease of handling, no need for additional chemicals, simple installation, high efficiency, and no need for sludge formation.

Extensive research on energy storage devices has been conducted in order to reduce the need for energy and achieve a sustainable environment. Metal oxide nanoparticles have also been used in environmental remediation as heterogeneous catalysts [26]. Nobel metals are not widely used as catalysts due to their limited availability and high cost, despite their extensive knowledge of catalytic oxidation of carbon monoxide [27]. Transition metal oxides have demonstrated superior catalytic oxidation properties [28].

Recently, different semiconductors and transition metal oxides such as g-C_3N_4, Fe_2O_3, CdS, TiO_2, Cu_2O, ZnO, MnO_2, WO_3, and CuO [29-31], have gained attention because of their good physical and chemical properties in terms of easy availability, and high activation. Despite having various characteristic properties to be used as photocatalyst, these materials lack at one or other points; like wide band gap (TiO_2 3.0-3.2 eV, ZnO 3.37 eV) [32,33], absorption in UV region, high photo-corrosion upon irradiation and instability in acidic and alkaline solutions. So, the quest of finding a metal oxide photocatalyst that possess superior photocatalytic activity in visible region has proposed CuO as a promising candidate with constricted band gap of 1.2-2.0 eV [34]. Moreover, CuO is cheap, easily available, have high surface volume, proper redox potential and excellent stability in solutions [34].

Apart from CuO nanostructures, various other materials as listed in Table 1 have been prospected by various researchers for the photocatalytic degradation of heavy metals considering the parameters like easy synthesis procedure, efficiency, and working pH range.

Table 1. Comparison of CuO modified catalyst with other materials for photocatalytic reduction.

S.No.	**Catalyst**	**Synthesis method**	**Pollutant**	**pH range**	**Result**	**Reference**
1.	CuO/TiO_2 nanocomposite	Sol-gel	Cr (IV)	4	Under visible light CuO and TiO_2 was optimum at a concentration of 0.5 wt%.	35

2.	Palygorskite modified with CuO	Precipitation	Cr (IV)	3-9	100% in visible light 10 mM tartaric acid over PAL/5.9CuO photocatalyst (400 mg/L)	36
3.	Flower like CuO	Microwave	Cr (IV)	3	100% *c*(Cr(VI)) = 100 μM, catalyst loading = 400 mg/L, *c*(tartaric acid) = 4 mM	37
4.	CuO/ZnO	Mechanical mixing	As (III)	neutral	Degradation is 6.5 times large in light than in dark	38
5.	CuO/ZrO_2-MCM-41 nanocomposites	In-situ incorporation	Cr (IV)	4	100% by 2 CuO@ZM-41	39
6.	CuO-Fe_3O_4	Co-precipitation	As (III)	7	118.11 mg/g	40
7.	CuO feather	Co-precipitation	Cr (III)	8	99.99% removal efficiency with 0.1 g adsorbent dosage	41

8.	3D iron-oxide	ultrasonication	As(V), Cr(VI)	neutral	25 times faster removal rate	42
9.	TiO_2–SiO_2	Sol-gel	Pb (II)	mild condition	98.6% removal efficiency with 3 g of catalyst	43
10.	Fe_2O_3-GQDs/NF-TiO_2	Electro-deposition	Cr (VI)		78% removal	44
11.	BiOI-Bi_2O_3 film	In-situ UV reduction	Cr (VI)		100% removal	45
12.	g-C_3N_4/TiO_2 NTs	Dip coating	Cr (VI)		99% removal	46
13.	Bi_2WO_6/mesoporous TiO_2 nanotube	One step solvothermal	Cr (IV)		3% BWO/TNTs remove Cr(VI) 3.8 times higher than BWO	47

These photocatalysts being used in wastewater reclamation by removing its organic, inorganic, and biological contaminants goes through five independent steps during the process [48]. These include (i) diffusion of pollutant molecules towards the surface of the catalyst particles from bulk solution, (ii) adsorption of these contaminants on the catalyst surface, (iii) generation of reactive radicals followed by decomposition of the pollutants, (iv) desorption of decomposed

products from catalyst surface, and (v) diffusion of these surface-desorbed decomposed products into the bulk of the reaction system, which are schematically illustrated in Figure 1.

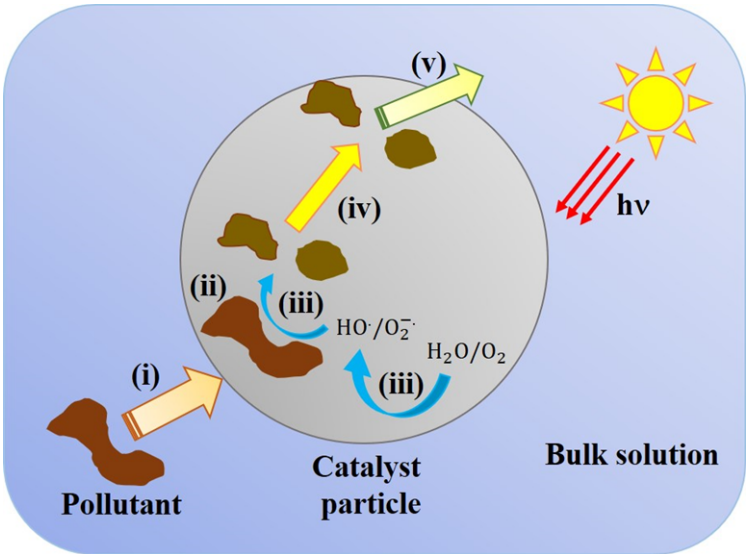

Figure 1. Schematic representation of photocatalytic degradation steps of organic pollutants on catalyst surface in aqueous solution. The catalyst particle size has been exaggerated to show reactions clearly.

The pollutants could affect human health by causing diseases or harming skin surfaces, disturb aquatic life via creating oxygen deficiency and make waterbodies unpleasant to use or destroy the natural aesthetic beauty or health of the water bodies. Pollutants may be classified into different types in terms of whether their consequences are known and there is already developed an analytical method of monitoring them. These include priority pollutants, emerging pollutants, and persistent organic pollutants. Priority pollutants are types of pollutants where their toxicity to humans and the environment is well established and for which there is already developed a method of analyzing and monitoring them. In terms of the health problems they induce in humans, organic water pollutants can also be categorized as endocrine disruptors, neurotoxins, teratogenics, and mutagenic and carcinogenic substances, Figure 2. The structural formula of some toxic organic pollutants is shown in Figure 3.

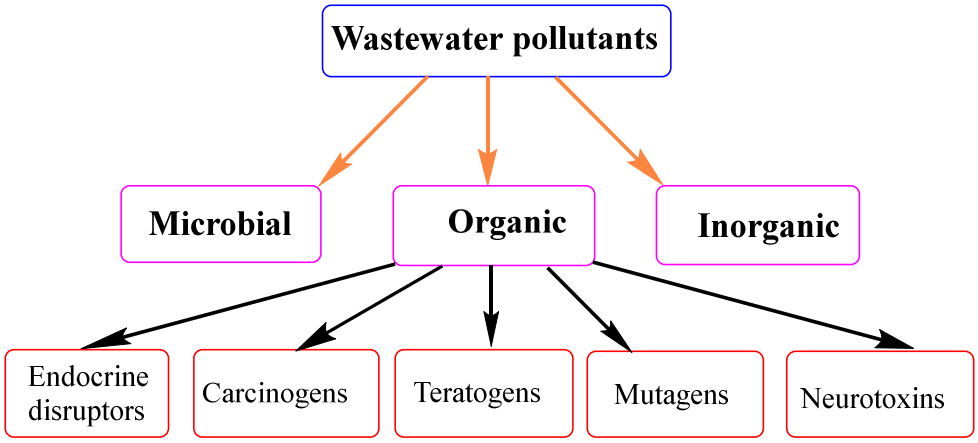

Figure 2. Classification of wastewater pollutants.

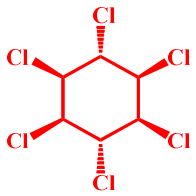

γ-Hexachlorocyclohexane,

Lindane (insecticide)

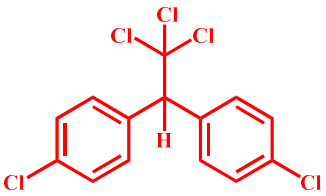

Dichlorodiphenyltrichloroethane,

DDT (pesticide)

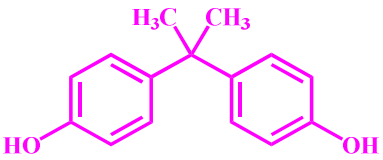

Bisphenol A **(plasticizer)**

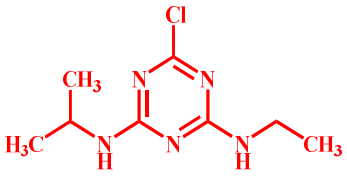

2-chloro-4-ethylamino-6-

isopropylamino-1,3,5-

triazine, **Atrazine**

(herbicide)

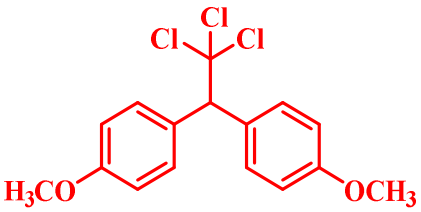

1,1,1-trichloro-2,2-

diphenylethane, **Methoxychlor**

(pesticide)

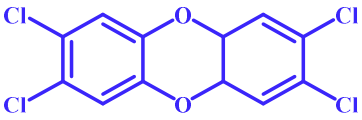

2,3,7,8-tetrachlorodibenzo-p-

dioxin, **TCDD (dioxins)**

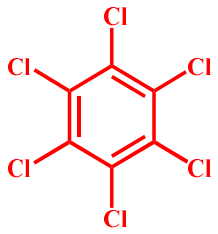

Hexachlorobenzene, **HCB**

(pesticide)

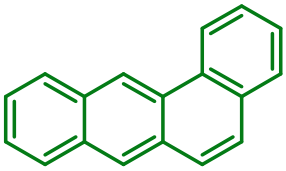

Benz[a]anthracene **(PCAHs)**

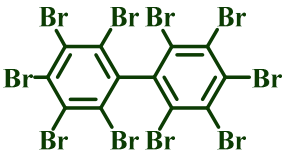

Decabromobiphenyl

(flame retardant)

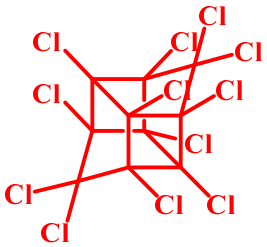

Mirex **(pesticide)**

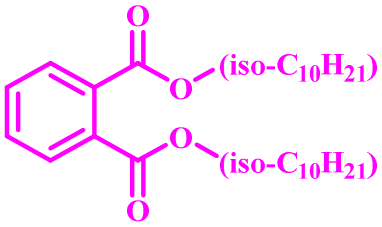

Diisodecylphthalate **(plasticizer)**

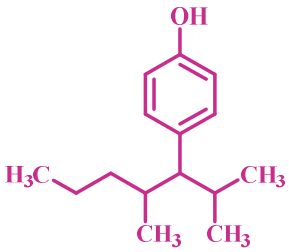

Nonylphenol **(surfactant)**

Figure 3. List of some toxic organic compounds and their structural formulae. Class of the pollutant is indicated in parenthesis; PCAHs = polycyclic aromatic hydrocarbons.

In that view, this review emphasizes the photocatalytic activity response of CuO catalyst for the factors influencing the efficiency of decontamination of the pollutants, and ways of mitigating the bottlenecks for effective removal are overviewed in detail and finally ends with a recap of the main points discussed.

2. Photocatalytic Mechanism of CuO Nanostructures

Photocatalysis is an alternative method which is used for the degradation of dyes in wastewater. The technique requires a high energy light irradiation source and an oxidant to generate hydroxyl radicals as the main process taking place is oxidation. In order to generate hydroxyl radicals responsible for the degradation of dye, electron-hole pairs are generated by irradiating the photocatalyst with a high energy light source. Electron-hole pairs are generated by

irradiating the photocatalyst with a high energy light source in order to generate hydroxyl radicals responsible for dye degradation. The photocatalytic process could be sped up by coupling it to a chemical process that converts the initial photo intermediate molecule to the final reactive species for wastewater treatment. This is accomplished through the homogeneous Fenton reaction, which generates reactive oxygen species in the presence of iron salts in aqueous media by decomposing H_2O_2. Photocatalytic reduction is currently in the process of transitioning from laboratory discovery to industrial application. It is ideal for demonstrating what is required to improve process performance in order for it to be adopted in industrial practice. Heterogeneous photocatalysis, which is one of the AOPs, can be defined as radiation–assisted acceleration of the rate of chemical reactions in the presence of semiconductor photocatalyst. Here, reactive radical species such as hydroxyl radical ($HO^{\cdot}$) and superoxide radical ion ($O_2^{-\cdot}$) are formed indirectly when energetic photons of incident radiation promote electrons from the valence band (VB) to the conduction band (CB) of the semiconductor, leaving holes behind in the VB and then the VB holes and CB electrons oxidize and reduce water and dissolved oxygen gas, respectively. The possible photocatalytic mechanism of CuO nanomaterials is proposed in Figure 4. As a photon with energy higher than the band gap energy of the semiconductor is adsorbed by the photocatalyst, electrons are excited from the valance band (VB) to the conduction band (CB) forming a hole. Generally, the generated charges recombine quickly and only a small fraction take part in the photodegradation of the pollutant resulting low photocatalytic efficiency. However, in the case of CuO the electron-hole pair path is different. Figure.5 schematic representation of the photocatalytic reduction of metal ions to elemental oxidation states.

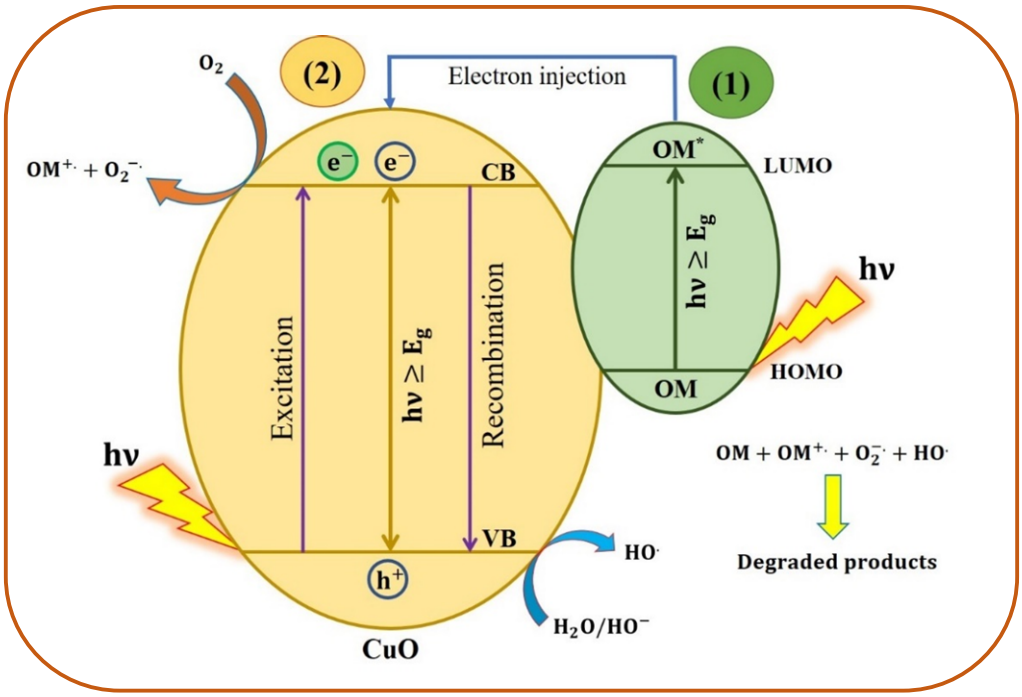

Figure 4. Illustration of general photocatalytic electron transfer and degradation reaction mechanism of organic pollutants.

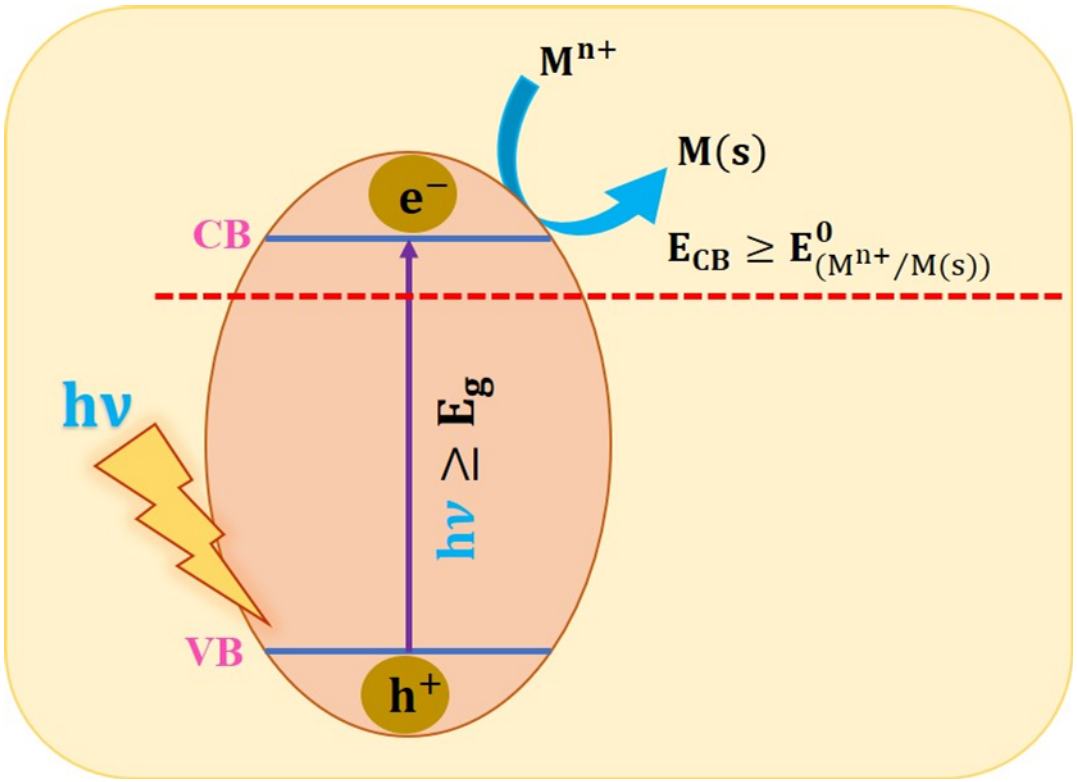

Figure 5. Photocatalytic reduction of metal ions to elemental oxidation states.

3. Effect of Parameters on the Photocatalytic Performance

Photocatalytic reduction is currently in the process of transitioning from laboratory discovery to industrial application. It is ideal for demonstrating what is required to improve process performance in order for it to be adopted in industrial practice. Following that, we will concentrate on the process parametrical space of the photocatalytic method, which will provide evidence of what is required to commercialize it. The effects of various operational parameters on the photocatalytic activity of CuO are also investigated, including catalyst loading, initial dye concentration, and dye solution pH are briefly discussed individually as follows.

3.1 Effect of pH

The solution pH is one of several factors that immensely affects the rate of heterogeneous photocatalytic degradation reaction of organic pollutants. It influences the reaction rate by affecting the charge of pollutant molecules and surface charge of the photocatalysts which in turn affects its adsorption capacity for the pollutant, the size of aggregated nanoparticles, the concentration of $HO^{\cdot}$ radicals, and the position of VB and CB edge potentials of the catalyst [49]. Pollutant adsorption to the catalyst surface is affected by the surface charge property of the catalyst particles which can be positive or negative depending on the pH of the media. The pH of zero point charge (pH_{zpc}) or also called isoelectric point (IEP) of a catalyst is the pH at which the net total surface positive and negative charges is zero at the operating conditions of experimental temperature, pressure, and solution composition [50]. At a pH greater than the pH_{zpc}, the surface charge of particles will be negative and adsorption of cationic pollutant molecules on catalyst surfaces will be favored. In contrast, at pH less than the pH_{zpc} surface charge will be positively charged and the adsorption of anionic pollutant molecules will be intensified. The pH_{zpc} value could depend on the nature of the photocatalyst and also on the synthesis method employed and for CuO synthesized using the microwave-assisted approach

the value was reported to occur at 8.5 which is determined using the zeta potential measurement method [51] and that other techniques such as the salt addition method [52] and potentiometric titration method [53] could also be used for measuring the pH_{zpc} of metal oxides. Several studies have reported the influence of pH on the removal efficiency of CuO and CuO-based catalyst towards organic pollutants. For example, Venkata *et al.* [54] studied the effect of varying pH from 3 to 11 on the degradation of methylene blue and Coomassie brilliant blue-250 dyes and found a maximum degradation percentage for both dyes individually at the optimum pH value of 7.

Banu *et al.* [55] investigated the influence of varying solution pH from 5 to 9 on the photocatalytic degradation proficiency of CuO/GO catalyst to brilliant green dye with other variables fixed and found an increasing tendency of degradation with pH till the optimal value at 7.5 and decreased afterward. They attributed this decreasing tendency at higher pH values to the poor adsorption of dye molecules on catalyst surface owing to a decrease in Coulombic attraction between cationic dye molecules and anionic catalyst surface in the presence of excess HO^- ions at such high pH values. In another study, Rao *et al.* [56] reported enhanced degradation of reactive black 5 dye at acidic pH of 3 achieving degradation of 90% compared to pH of 7.5 and 11, achieving removal efficiency of 76 and 53%, respectively over the same time duration and similar other experimental parameters. The reason for the higher removal at lower pH was similarly ascribed to the facilitated adsorption of cationic CuO NPs and anionic dye molecules which results in a fast rate of degradation. Moreover, a decrement in the degradation of aniline in water upon increasing pH above the neutral value was observed using CuO NPs catalyst in a report by Norzaee *et al.* [57] and similarly explained the phenomenon as described above. Chauhan *et al.* [51] studied the degradation of Victoria blue dye at acidic, basic and neutral pH values using CuO NPs photocatalysts and found a maximum degradation percentage at the basic pH of 10. According to the authors, the higher activity rate of the

catalyst is due to favored adsorption of cationic dye molecules with the anionic surface of the catalyst for media pH was higher than pH_{zpc} of the catalyst measured to be 8.5. Table 1 gives a range of pH where the degradation percentage of various pollutants using CuO and CuO-based catalysts was measured and the optimum pH where the highest rate of elimination of different organic pollutants was observed.

Table 1. Effect of solution pH on degradation percentage of various organic pollutants using CuO and CuO based catalysts. Key: Gr = graphene, RhB = Rhodamine B, CP = Clinoptilolite, ZIF-8 = zeolitic imidazolate frameworks -8, LP = low pressure, RB = reactive black,

Catalyst	Pollutant (ionicity)	pH range measured	Optimum pH	Other conditions	D (%)	Ref.
CuO	Aniline (neutral)	3 – 11	7	Catalyst dose = 0.05 g/L, aniline conc. = 100 mg/L, t = 60 min, using UV light	78	[57]
CuO	Phenol (neutral)	2 – 13	4 – 7	Catalyst dose = 0.05 g/L, phenol conc. = 0.25 g/L, 0.1 M H_2O_2, t	100	[58]

				= 35 min., using UV light		
Co/Ag/CuO	Methyl orange (anionic)	3 – 11	7	Catalyst dose = 0.1 g, MO conc. = 0.02 mM, using 50W xenon lamp	87.54	[59]
Fe_2O_3/Gr/CuO	Methylene blue (cationic)	1 – 11	9	Catalyst dose = 0.5 g/L, MB conc. = 20 mg/L, using 100 W visible light	78.8	[60]
ZnO/CuO/rGO	RhB (cationic)	3 – 12	11	Catalyst dose = 0.1g, RhB conc. = 5ppm, using visible light	99	[61]
CuO	Textile wastewater	3 – 11	6.9	Catalyst dose = 0.05 g/L, t	83	[62]

				= 1h, using UV light		
CuO	Direct red 81 (anionic)	2 – 10	4	Catalyst dose = 0.03 g, Direct Red 81 conc. = 0.1 mM, using UV-vis light	~90	[51]
Fe_3O_4@CuO	Congo red (anionic)	4 – 11	4	Congo red conc. = 30 mg/L, using sunlight	___	[63]
CuO	Phenol (neutral)	4 – 8	6	Catalyst dose = 0.02g, Phenol conc. = 100 mg/L, t = 1 h, using sunlight	~ 100	[64]
CuO-CP	p-aminophenol (neutral)	2 – 11	6	Catalyst dose = 2 g/L, p-aminophenol conc. 20	~ 60	[65]

				mg/L, using sunlight		
CuO	Rhodamine B (cationic)	1 – 14	7	Rhodamine B conc. = 10 ppm, using UV light	90.73	[66]
CdS-CuO	Methylene blue (cationic)	3 – 10	5	Catalyst dose = 0.8 g/L, MB conc. = 1 ppm, t = 80 min., under Hg-lamp	83	[67]
CuO	Metronidazole	3 – 11	3	Catalyst dose = 8 mg/L, metronidazole conc. = 50 mg/L, H_2O_2 = 10 mL, t = 1h	98.36	[68]
CuO	λ -cyhalothrin (L-CHT) (insecticide)	5 – 9	7	Catalyst dose = 2 mg/L, L-CHT conc. = 20 ppm, t =	98	[69]

				3h under UV irradiation		
5Wt%CuO/ZIF-8	Rh6G	5 – 12	12	Catalyst dose = 25 mg, Rh6G conc = 12.5 ppm, t = 105 min., under sunlight	~ 99	[70]
CuO	Congo red	2 – 12	2	Catalyst dose = 0.05 g, Congo red conc. = 10 g/L, t = 60 min. under UV light	85	[71]
CuO	RhB	2 – 12	10	Catalyst dose = 0.05 g, Congo red conc. = 10 g/L, t = 60 min. under UV light	94	[71]

ZnO/CuO	RhB	4, 7, and 11	11	Catalyst dose = 100 mg, RhB conc. = 10 ppm, t =100 min., 125W LP Hg lamp	~ 100	[72]
10wt%CuO/$SmFeO_3$	RhB	3 – 11	5	Catalyst dose = 0.15 g, RhB conc. = 8 ppm, t = 300 min., under visible light	65	[73]
CuO	RB-5	3, 7.5, 11	3	Catalyst dose = 20 mg, RB-5 conc. = 0.02 mM, t = 30 min. under visible light	90	[56]
CuO/Bi_2O_3	Methylene blue	3 – 11	3	Catalyst dose = 0.2 g/L, Methylene blue conc. = 10 ppm, t = 2	87.87	[74]

				h under UV-C light		

3.2 Effect of temperature

The temperature of the reaction mixture has also an impact on the rate of degradation of organic pollutants during water and wastewater treatment. The rate of photocatalysis is expected to increase with temperature in accordance with Arrhenius theory which states that the apparent reaction rate constant increases with exp(-1/T). In general, with the rise in reaction temperature photocatalytic degradation of organic pollutants can be enhanced due to [75,76] (i) increased oxidation rate at the solid-solution interface, (ii) suppression of charge carrier recombination, and (iii) increase in the number of cavitation bubbles which promotes the formation of free radicals. However, at temperatures close to the boiling temperature of the solvent, pollutant elimination proficiency could be dropped as in this case the reaction is limited by the lowered rate of adsorption and hence temperature range of 20 – 80 ^{o}C has been regarded as optimum for achieving maximum decomposition efficiency [77].

Very few reports are available in the literature about the influence of reaction temperature on the degradation of organic pollutants using CuO and CuO-based photocatalysts. For instance, Nuengmatcha *et al.* [78] found better decomposition of methylene blue dye using Fe_2O_3/graphene/CuO ternary composite at a temperature of 40 ^{o}C. They stated that the rate of degradation reaction increased on increasing the temperature from 10 ^{o}C to 40 ^{o}C, indicating the endothermic nature of the reaction, however, raising the temperature further to 50 ^{o}C lowered the degradation and this could be due to the higher recombination rate of e^{-}/h^{+} pairs at this temperature. On the contrary, keeping other parameters unchanged, a consistent increase in the degradation of rhodamine B dye using biosynthesized CuO NPs under UV light

irradiation in the temperature range from 30 – 70 ^{o}C was observed, reaching a maximum of 85% at 70 ^{o}C as reported by Rafique *et al* [79]. The researchers explained this rise of degradation with temperature to be due to rise in reactive surface sites with temperature which results in increase in the number of reactive radicals and hence rate of decomposition rate of the dye. In a similar study by the authors, about 95% removal performance of RhB dye by biosynthesized CuO NPs at 80 ^{o}C was reported when the temperature was varied from 30 – 80 ^{o}C while other operational parameters are maintained at fixed values and similar explanation as above was offered to the observed phenomenon [80]. In a study conducted by Acedo-Mendoza *et al.* [81], enhanced photocatalytic degradation of methylene blue and methyl orange dyes taken individually was reported up on increasing the reaction temperature from 25 to 45 ^{o}C, reaching respective decomposition percentages of 99% after 15 and 75 minutes of exposure under UV light employing CuO supported on ZnO catalyst. The authors suggested that the reason for the augmented rate of degradation was because of the endothermic nature of the adsorption process of the dyes onto the surface of catalyst particles which increases with temperature rise. Therefore, during heterogeneous photocatalytic degradation reactions, the temperature of the reaction mixture has to be maintained to avoid its likely interference when comparing the removal competence of catalysts for organic pollutants.

3.3 Effect of aeration and stirring rate

Aeration and rate of stirring are two other factors that can significantly influence the rate of photodegradation reactions. Dissolved oxygen in solution impacts the rate of photocatalysis by accepting photoexcited CB electrons to give $O_2^{-\cdot}$ and subsequently $HO^{\cdot}$ via Eqs. (1-4) and thereby separating the photogenerated e^-/h^+ pairs. Thus, aerating the reaction mixture could boost degradation by not only supplying molecular oxygen to the solution and fostering its reduction on surfaces of catalyst particles, which is a rate-determining step but also assisting mass transfer by turbulence [82].

$$O_2 + e^- \rightarrow O_2^{-\cdot} \quad (1)$$

$$O_2^{-\cdot} + H^+ \rightarrow HOO^{\cdot} \rightarrow H_2O_2 \quad (2)$$

$$H_2O_2 + e^- \rightarrow HO^- + HO^{\cdot} \quad (3)$$

$$H_2O_2 + O_2^{-\cdot} \rightarrow HO^- + HO^{\cdot} + O_2 \quad (4)$$

Moreover, stirring of the reaction mixture simultaneously during photocatalytic degradation could increase the rate of reaction by enhancing the dissolution of oxygen in solution through the turbulent motion of the solution and increasing the rate of movement of dye molecules to the catalyst surface from the bulk by increasing the rate of diffusion and mass transfer mechanisms [83]. However, at and above a certain stirring speed, the rate of reaction becomes no longer dependent on it and exhibits no further improvements in degradation as observed in the case of the degradation of 4BS azo dye using TiO_2 NPs as photocatalyst [84].

3.4 Effect of energy and intensity of radiation

Photocatalytic degradation reactions of organic pollutants are also prominently influenced by the energy and intensity of the radiation source. While the intensity of radiation refers to the number of photons that pass per unit area per unit time, energy is related to the wavelength of the radiation and that the shorter the wavelength or the higher the frequency the higher the energy of the radiation. Therefore, for feasible and reasonable heterogeneous catalysis reactions to occur, incident radiation should be first of all energetic enough to induce excitation of VB electrons to the CB of the semiconductor catalyst and that it should also have sufficient enough intensity to form more charge carriers and higher reactive species to run the decomposition process. Generally, at a lower intensity of radiation input from 0–20 W/cm^2, the reaction rate increases linearly with intensity whereas it increases with square root dependence at the moderate regions of intensity [85]. However, after a certain threshold value, the reaction

rate remains constant regardless of intensity for saturation point of catalyst surface with photoproduced charge carriers has reached which results in mass transfer limitation in the adsorption-desorption process, preventing the interference of light intensity in the rate of the reaction [48].

Some researchers have studied the influence of energy and intensity of radiation sources on the photocatalytic removal of organic contaminants using CuO-based photocatalysts. For example, Zeid *et al.* [59] found out that the chemical oxygen demand (COD) removal of methyl orange dye during a degradation time conducted for 2 h in the presence of Co/Ag/CuO catalyst and using 50 W Xenon lamp, 80W UV-lamp, and sunlight was quite different, with their respective removal efficiencies of 91, 71, and 62 % over the same mentioned time duration. In another study, COD removal of 83.8, 93.2, and 98.9% of the antibiotic ciprofloxacin hydrochloride using lamps of intensities 8, 15, and 30 W and pollutant concentration of 11.2 mg/L, CuO catalyst dosage of 0.08 g/L, and pH of 8.17 under ultraviolet light was reported by Khoshnamvand *et al* [86]. Moreover, it has also been reported that the degradation of methylene blue using radiation of intensity varying from 40 to 100W increased degradation from 25% to 60% but increasing the intensity further to 130W did not result in a significant increase in the percent removal of the dye [77]. A pronounced variation in the degradation of methyl orange in the presence of Ag/CuO catalyst and under visible and ultraviolet light radiation sources while keeping other parameters unchanged was also reported by Khan *et al* [87].

3.5 Effect of the presence of oxidants and other interferants

Oxidants are substances that oxidize other reactant species by accepting electrons. They are sometimes deliberately added into photocatalytic reaction systems to speed up the rate of reaction. The hydroxyl radical ($HO^{\cdot}$) is the most common oxidant with an oxidation potential

of +2.8V vs NHE which oxidizes many organic compounds non-selectively [88]. Depending on the nature of the organic pollutant, it can attack the pollutant via four mechanisms, namely hydrogen abstraction, electron transfer, radical addition, and radical combination [89]. It can be produced by adding hydrogen peroxide (H_2O_2), which produces $HO^{\cdot}$ by reacting with CB electrons, Eq. (5) or via direct photolysis, Eq. (6)

$$H_2O_2 + e^-(CB) \rightarrow HO^{\cdot} + HO^- \quad (5)$$

$$H_2O_2 + h\nu \rightarrow 2HO^{\cdot} \quad (6)$$

Other oxidants used include sulfate radical ion ($SO_4^{-\cdot}$), produced from the addition of persulfate ($S_2O_8^{2-}$) salts or peroxomonosulfate (HSO_5^-) or oxone, permanganate (MnO_4^-), and chlorine dioxide (ClO_2) with their respective oxidation potentials of +2.5-3.1, +1.7, and +1.5 V vs. NHE [90]. Different researchers have studied the influence of adding oxidants on the photocatalytic degradation of organic pollutants. For instance, Mukwevho *et al.* [91] observed enhanced degradation of phenanthrene in the presence of 2mM $K_2S_2O_8$ and ascribed the increase in decomposition owing to the effective separation of e^-/h^+ pairs and also the formation of $HO^{\cdot}$ radical via reactions in Eq. (7-9),

$$S_2O_8^{2-} + e^-(CB) \rightarrow SO_4 + SO_4^{-\cdot} \quad (7)$$

$$SO_4^{-\cdot} + e^-(CB) \rightarrow SO_4^{2-} \quad (8)$$

$$SO_4^{-\cdot} + H_2O \rightarrow SO_4^{2-} + H^+ + HO^{\cdot} \quad (9)$$

In another study, Sharma and Dutta [92] reported striking improvement in the degradation of acid orange-74 dye using triphenylphosphine oxide capped CuO nanoparticles in the presence of H_2O_2 and $K_2S_2O_8$ oxidants and this was explained in terms of the successful separation of e^-/h^+ pairs due to their excellent electron capturing ability. In addition, Abdullah *et al.* [93] also reported a similar significant increment of degradation in the presence of the

optimum amount of H_2O_2 for the degradation of reactive orange 16 using CuO nanoparticles. On the other hand, Hong *et al* [94] stressed the importance of adding only an appropriate amount of H_2O_2 for resulting in maximum degradation of rhodamine B (RhB) using CuO/g-C_3N_4 photocatalyst. They stated that adding 100μL of 30% H_2O_2 to a reaction system containing 10 mL of 0.01 mM of RhB and 0.01 g of catalyst loading under 300W Xenon lamp resulted in a higher rate of degradation but utilizing 200 μL or 50μL inhibited the removal rate and ascribed this to the insufficient amount of oxidant to induce the Fenton-like reaction at lower concentration and to the $HO^{\cdot}$ scavenging effect of H_2O_2 at higher concentration to give the weaker oxidant $HOO^{\cdot}$ and O_2 gas.

As typical industrial wastewater is a cocktail of chemicals, studying the effect of other interferents than target pollutants on the photocatalytic activity of a catalyst is also highly essential. These interfering substances can be not only those which exist along with the target pollutant before degradation commences but also intermediate products formed in-situ during the degradation process and tend to lower degradation efficiency by fouling the catalyst [95]. Generally, while inorganic ions may inhibit the rate of degradation by competing for adsorption with target molecules or acting as radical scavengers, other organic pollutants than the targets lower efficiency by undergoing co-degradation. The most common inorganic ions available in wastewater include Cl^-, NO_3^-, PO_4^{3-}, SO_4^{2-}, CO_3^{2-}, and HCO_3^-. In the dying process in the textile industry, NaCl is added to facilitate the diffusion of dye molecules and their adsorption onto fabrics whereas CO_3^{2-} and HCO_3^- are used to enhance the fixation ability of the dye molecules onto the fibers of the fabrics [96]. These ions acting individually may fasten, retard or have no or little effect on the rate of photocatalytic degradation of organic pollutants in wastewater. On other hand, they can retard the rate of degradation by competing for catalyst surface adsorption with the contaminant molecules and poisoning or coagulating it or serving as radical scavengers thereby decreasing the concentration of active radical species and rate of

degradation. In contrast, they can also fasten the rate of reaction via forming additional reactive radicals in the reaction medium.

There are a limited number of reports emphasizing the influence of interferents during the degradation process of target organic contaminants using CuO or CuO-based nanoparticles. For instance, the retarding effect of the addition of CO_3^{2-} and HCO_3^- and Cl^- individually on the degradation of methylene blue under 35W Hg-lamp using NiO/CuO catalyst was reported by Senobari *et al.* [97]. This inhibition was proposed to be due to their $HO^{\cdot}$ scavenging properties to give weaker carbonate and chloride radicals, thereby suppressing the extent of decomposition rate. In another study, it was found that the degradation of tetracycline was immensely reduced in the presence of SO_4^{2-}, NO_3^-, and Cl^-, with the extent of reduction in the order of the list of the ions, using N-doped carbon embedded with CuO particles [98]. However, significant enhancement in the kinetics of reaction for the photocatalytic decomposition of bisphenol A using $CuO/Fe_2O_3/ZnO$ composite in the presence of SO_4^{2-}, Cl^-, and PO_4^{3-} as opposed to the ions CO_3^{2-} and NO_3^-, which in their presence the degradation reaction kinetics was inhibited under visible light irradiation [99]. It was suggested that while the enhancement could be due to the formation of secondary radicals, the suppression was proposed to be due to radical formation inhibition by competing for surface adsorption and radical scavenging effects. In another study, Wang *et al.* [100] studied the influence of adding NO_3^-, SO_4^{2-}, Cl^-, and HCO_3^- anions on the photocatalytic degradation performance of 13.4wt%CuO/g-C_3N_4 heterojunction photocatalyst for the degradation of the antibiotic oxytetracycline in the presence of peroxymonosulate as an activator. They discovered that, except for SO_4^{2-}, which had little effect on the degradation process, the rest of the anions slowed the rate of decomposition. This hindrance was attributed to the trapping effect of the anions to the $HO^{\cdot}$ and $SO_4^{-\cdot}$ and holes reactive species to produce radical species with lower redox

potentials, that is $HO^{\cdot}$ and $SO_4^{-\cdot}$ react with NO_3^-, Cl^-, and HCO_3^- anions to produce the less reactive $NO_3^{-\cdot}$, $Cl^{-\cdot}$, and $HCO_3^{-\cdot}$ radicals, respectively.

The addition of the reducing substance sodium borohydride ($NaBH_4$) to the photocatalytic degradation reaction system also augments rate of reaction. For instance, the degradation of Allura red dye was fastened using porous CuO nanosheets as photocatalysts in the presence of $NaBH_4$ as reported by Nazim *et al.* [101]. As stated by the authors, the enhanced decomposition of the dye is due to the reducing ability of $NaBH_4$ to dissolved oxygen in solution and subsequent generation of reactive oxygen radicals, $O_2^{-\cdot}$ and $HO^{\cdot}$, Eq. (10-12).

$$NaBH_4 \rightarrow Na^+ + BH_4^- \rightarrow BH_3 + H^+ + e^- \quad (10)$$

$$O_2 + e^- \rightarrow O_2^{-\cdot} \quad (11)$$

$$O_2^{-\cdot} + H_2O \rightarrow HO^{\cdot} + HO^- \quad (12)$$

Similar dramatic disappearance in the color of rhodamine B using CuO/PVA [102] and Congo red and methylene blue taken both individually and their mixtures using biosynthesized CuO NPs in the presence of $NaBH_4$ [103] was also observed.

3.6 Effect of supports

Particle aggregation is one problem that lowers the photocatalytic degradation efficiency of catalysts for organic contaminants when they are applied in slurry form. Therefore, to overcome this problem, active catalysts are synthesized in the presence of support compounds to add the benefits of uniformly spreading the active photocatalysts, enhancing the adsorption capacity for pollutant compounds and their intermediate products, and promoting the recyclability and separation of charge carriers [48]. Substances used in such application include zeolites ($Na_2Al_2Si_2O_8$), silica (SiO_2), activated carbon, bentonite ($Al_2H_2Na_2O_{13}Si_4$), Kaolinite ($Al_2O_3.2SiO_2.2H_2O$), mordenite ($(Na_2, Ca, K2)_4(Al_8Si_{40})\ O_{96}\cdot 28H_2O$), g-$C_3N_4$, graphene,

reduced graphene oxide, chitosan, etc. The supports can play either only a supporting role and cannot generate e^-/h^+ pairs or can play both supporting roles while at the same time actively involving the generation of charge carriers and therefore are semiconductors. Some reports in the literature utilized supports along with the active catalyst CuO or CuO based catalyst for the photocatalytic degradation of organic pollutants in water and wastewater. For instance, a far more enhanced rate of degradation of CuO supported on nano clay particles compared to pure CuO for the degradation of methyl orange was reported by Khan *et al* [104]. According to the authors, the enhanced performance of the CuO/nanoclay composite is due to the uniform deposition of CuO particles on nanoclay particles which increases its surface area and synergistic effect in reducing recombination of charge carriers. Significant improvement in the photocatalytic decomposition of methylene blue using chitosan-CuO hybrid catalyst compared to pure CuO in the presence of a small amount of H_2O_2 was also observed by Haldorai and Shim [105]. The higher catalytic activity of the catalyst was due to the formation of the hybrid which increased the adsorption of the dye and improved the self-regeneration and easy separation of the catalyst from the aqueous solution. A study of the removal of 2,6-Dimethyl phenol using CuO-Clinoptilolite composite showed an increased rate of degradation in comparison to pure CuO and was proposed to be due to the distribution of CuO particles on the zeolite particles thereby increased surface area of the photocatalyst [106]. Comparison of the degradation of Congo red dye using pure CuO and 1wt% CuO supported on eggshell (1wt%CuO/eggshell) catalysts under visible light for a period of 4 h and at similar other parameters showed an insignificant difference, that is 82% versus 80%, respectively [107]. It was proposed that the structural features and the correlation between the support eggshell and the active catalyst CuO gave rise improved rate of degradation and this strategy are also economically beneficial for the consumption of active catalysts can be lowered without causing significant loss in degradation efficiency.

There are several traditional methods of toxic metal ions removal techniques such as chemical precipitation, membrane filtration, electrochemical reduction, adsorption, coagulation, flocculation, flotation, etc. However, the disadvantage with these methods is that they are environmentally unfriendly and can produce huge sludge during treatment which incurs an additional cost of processing and transportation [108]. Photocatalytic redox method is the removal of the toxic metal ions by changing to their metallic elements, metal oxides or converting their valence to non-toxic or lower toxicity via oxidation or reduction reactions and offers such advantages as environmentally friendliness, ease to handle, no need to utilize large chemicals, easy to install, significant efficiency and does not involve the formation of sludge as compared to the traditional treatment approaches [109].

4. Analysis of real samples using CuO modified electrodes as photocatalysts

Detection of heavy metals, dyes, pesticides using nanocomposite modified electrodes as photocatalyst has gained importance for environmental protection from toxins and pollutants. A. M. *et. al.* [110] have fabricated $CuO/MnO_2/Gd_2O_3$ ternany nanomaterials for the detection of industrial effluent (collected from the Jeddah Industrial Area, Saudi Arabia) and extracted samples out of them. $CuO\text{-}TiO_2$ modified GCE was used for sensitive and selective detection of methyl parathion (MP) pesticide in ground water obtained from Jianghan Plain, Hubei, China [111]. In this study the recovery of MP ranges from 98.80% to 106.70% in the real water samples. Furthermore, scientists have comparison the detection limits of bicarbonate in the real samples taken from different water sources using CuO-ZnO NRs/AgE as electrochemical sensing electrode which come out be 0.89 ± 0.02 nM [112]**.** Chemical sensor based on Ag_2O/CuO NSs/binder/GCE was used to detect 2-NP in real environmental sample with the detection limit of 3.31 ± 0.17 pM [113].

Bajiri *et al* [114] studied the photocatalytic performance of CuO/ZnO/g-C_3N_4 ternary composite for the photocatalytic degradation of methylene blue under visible light illumination. They found about 98% removal efficiency at 45 minutes of degradation time using 100 mL of 10 ppm methylene blue and 0.04 g of catalyst and 400W hollow lamp as a light source. The authors proposed that the observed pronounced activity of the ternary composite as compared to CuO/ZnO binary composite was due to efficient separation of photogenerated e^-/h^+ pairs by the Z-scheme charge carrier transfer mechanism, Figure 6, rather than the conventional type II heterojunction structure.

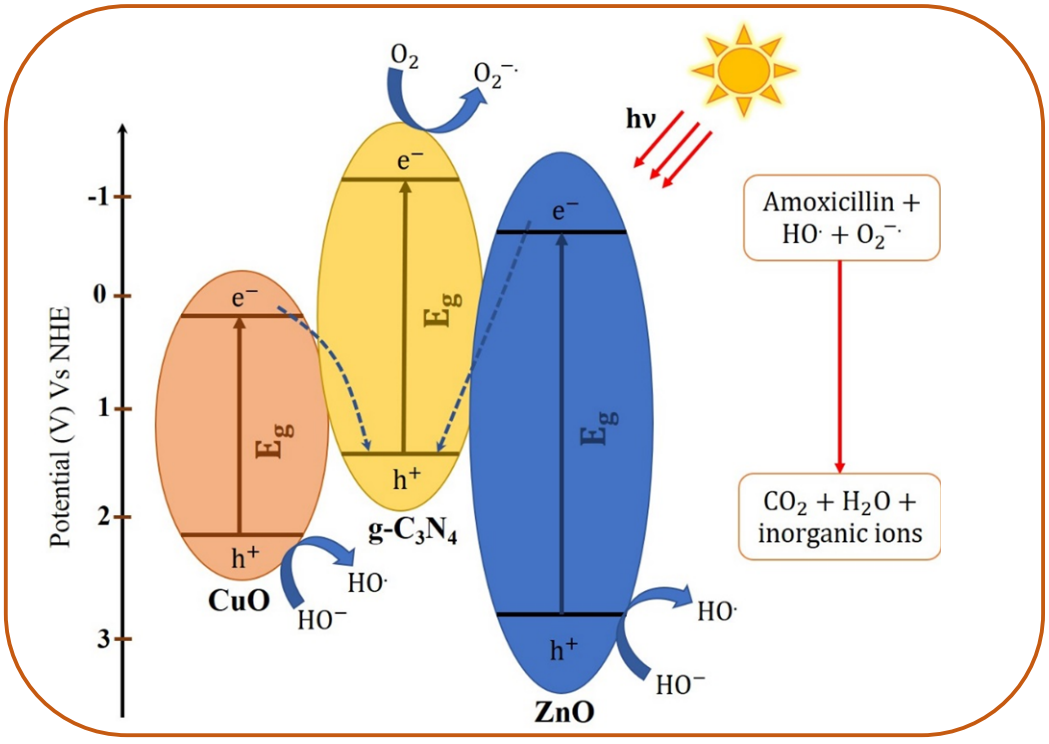

Figure 6. Band position potential and Z-scheme charge transfer mechanism in CuO/ZnO/g-C_3N_4 composite during the degradation of Amoxicillin. Reprinted with permission from reference [114].

5. Effect of Parameters on the Decontamination of Toxic Heavy Metal Ions via Photocatalytic Degradation

Just as organic pollutants, the degree of photocatalytic removal of toxic heavy metal ions from aqueous solution is impacted by such factors as solution pH, energy and intensity of the radiation source, catalyst dose, metal ion concentration, and morphological properties of the photocatalyst employed. These factors are briefly discussed individually as follows.

5.1 Effect of energy and intensity of radiation

Different researchers have studied the influence of energy of radiation sources on the removal of heavy metal ions using CuO-based catalysts. For example, Ravishankar *et al.* [35] found that the photocatalytic reduction of Cr^{6+} to Cr^{3+} using CuO/TiO_2 in the presence of CuO/TiO_2 composite catalyst under sunlight illumination for a contact time of 80 minutes was higher than under UV lamp.

5.2 Effect of catalyst loading

The amount of catalyst employed also affects the amount of metal ions to be removed from the aqueous solution. The higher the amount of catalyst, the greater the number of surface-active sites to form more conduction band electrons and higher will be the reduction rate of nearby metal ions. Few researchers have reported the impact of CuO and CuO-based catalyst loading on the removal percent of toxic heavy metal ions. For instance, Xu *et al.* [36] studied the influence of raising the amount of palygorskite/CuO catalyst loading from 200 to 1600 mg/L for the photocatalytic removal of Cr(VI) from aqueous solution and removal rate increased with catalyst dose, though the final 800 mg/L and 1600 mg/L loadings did not produce very much difference in removal efficiency. The effect of varying CuO NPs dosage from 200, 400, 800, and 1600mg/L on the photoreduction of Cr(VI) in the presence of tartaric acid was also studied [37]. The result indicated that the removal of the metal ion increased when catalyst loading was raised from 200 to 400 mg/L but any further increase to 800 and 1600 mg/L resulted in a reduced rate of elimination and the reason for the first case was

attributed to the associated increase in the number of active sites for adsorption and reduction of the metal ion but for the later it was ascribed to the formation of the turbid solution by the excessive amount of catalyst which obstructs radiation and hence suppressed generation of charge carriers and rate of removal of metal ions.

In another study, Samad *et al.* [38] investigated the impact of varying the CuO/ZnO catalyst loading from 0.33, 0.67, and 1.00 g/L to the photocatalytic oxidation of As(III) to As(V) and they found the removal rate increases with the rise in catalyst dose and observed complete removal of the ion using 1.00 g/L of the catalyst in 8h of illumination under UV light. The authors have ascribed the increase in the removal of the metal ion with an increase in catalyst dose to be due to the associated increase in the number of surface-active sites with catalyst amount.

5.3 Effect of pH

The pH of media affects the reduction of metal ions by modifying the CB and VB edge potentials of the semiconductor. However, only Cr^{6+} exhibits a pH-dependent shift in the VB and CB edge potentials and therefore the photocatalytic reduction of many of the toxic metal ions is pH-independent because the CB edge potentials of the ions are more positive than the redox potential of the ions [115]. Nanda *et al.* [39] studied the influence of varying suspension pH from 4–10 on the photocatalytic reduction of Cr^{6+} using CuO/ZrO_2-MCM-41 composites as photocatalysts. They found around 80% reduction of the metal ion at pH of 4 using 1 g/L catalyst dose and 20 ppm of Cr^{6+} initial concentration under solar light irradiation for 30 minutes. The authors attributed the higher reduction rate at acidic than alkaline pH to the greater adsorption of $HCrO_4^-$, which Cr^{6+} predominantly exists at acidic pH, to the positively protonated charged catalyst surfaces of the particles because the suspension pH of 4 was greater than the pH_{zpc} measured to be 4.5. The influence of varying pH and reaction time at constant

CuO/Kaolin catalyst loading of 2 g/L and Cr(VI) initial concentration of 30 mg/L while keeping other parameters the same was studied by Mohagheghian *et al.* [116] using response surface methodology. The reduction efficiency was increased with increasing reaction time and decreased with increasing pH of the suspension from 3 to 9 and nearly complete removal (99.99%) was achieved at pH of 3 for 2 h of reaction time. The pH_{zpc} of the CuO/Kaolin catalyst was determined to be nearly 7.3 and reasoned that the higher removal performance of the catalyst at lower pH is due to the favored adsorption of anionic compounds such as CrO_4^{2-} and $HCrO_4^-$ on the positively charged CuO/Kaolin composite at such pH which leads to improved reduction of Cr(VI). The authors further forwarded that Cr (VI) is reduced to Cr(III) in acidic and neutral conditions whereas Cr(III) is precipitated to $Cr(OH)_3$ in alkaline condition, Eq. (13– 15),

$$Cr_2O_7^{2-} + 14H^+ + 6e^- \rightarrow 2Cr^{3+} + 7H_2O \text{ (acidic environment)} \quad (13)$$

$$CrO_4^{2-} + 8H^+ + 3e^- \rightarrow Cr^{3+} + 4H_2O \text{ (neutral environment)} \quad (14)$$

$$CrO_4^{2-} + 4H_2O + 3e^- \rightarrow Cr(OH)_3 \downarrow + 5HO^- \text{(alkaline environment)} \quad (15)$$

A removal percentage of about 90% for As(III) was achieved in the pH of 4 to 8 via photooxidation to As (V) followed by adsorption utilizing CuO-Fe_3O_4 nanoparticles as photocatalyst and this was superior to only 20% achieved at a pH of 9 to 12 [40].Therefore, the operating pH of the solution significantly affects the photocatalytic redox reaction and hence needs to be optimized to achieve maximum elimination efficiency in addition to other parameters.

5.4 Effect of initial metal ion concentration

The initial metal ion concentration also significantly affects its percentage removal by a photocatalytic redox reaction in the presence of photocatalysts. The percent removal of the metal ion is given by Eq. (16),

$$\text{Removal } (\%) = \left(\frac{C_0 - C_t}{C_0}\right) \times 100 \quad (16)$$

Where, C_0 and C_t refer to the initial concentration of the contaminant ion before exposure to radiation and after exposure time t, respectively. In general, as the concentration of metal ion increases, its removal percentage decreases after a certain threshold value in which a saturated state in the number of active sites of the photocatalyst has reached because the amount of catalyst is constant as contaminant ion concentration is raised. The impact of varying the initial Cr^{6+} concentration from 2 – 50 mg/L on its photocatalytic reduction using CuO/ZrO_2-MCM-41 was studied and result found indicated that initially when 2 – 5 mg/L was used nearly 100% elimination was observed meanwhile the removal percentage went decreasing afterwards with efficiency of only 43% when 50 mg/L was employed [39]. This has been proposed to be owing to the increased light absorption as the concentration of metal ion is increased while the number of active sites is the same, resulting in hindered generation of photogenerated e^-/h^+ pairs and photoreduction of the metal ion. Similar lowered rate of removal of Cr(III) with rise in its concentration from 50 – 450 mg/L using CuO photocatalysts with different particle morphologies under UV-C irradiation was reported and similar explanation as stated above has been offered [41].

6. Conclusion

In this review, the effect of operational parameters such as catalyst dose, pH of suspension, energy and intensity of radiation, stirring rate, pollutant initial concentration, temperature, presence of other co-contaminants or deliberately added oxidants to facilitate the degradation reactions on CuO nanostructure have been discussed in detail as they predominantly affect the photocatalytic decomposition rate. Lower or higher catalyst loading than the optimum amount could result in an inhibited rate of degradation percentage because the number of photogenerated reactive radicals responsible for the decomposition of organic pollutants is suppressed owing to the reduced number of surface-active sites and scattering of radiation by suspended particles at a lower and higher amount, respectively. Similarly, the initial dye concentration used compared to the amount of catalyst dose should be balanced; if higher than optimum organic pollutant concentration is used then the incident radiation will be absorbed by the molecules of the pollutant, resulting in minimized photogenerated charge carriers' generation and rate of reaction. Regarding pH, photocatalyst should have pH_{zpc}. Above this value, the surface of the catalyst particles will be negatively charged which favor the adsorption of positively charged contaminant molecules, and below it, the positively charged calayst particles will facilitate the adsorption of anionic molecules and hence enhances the removal percentage. The other operational factors specified in this review have also their influence on the efficiency of degradation, and optimizing them is essential to achieve maximum elimination of the contaminants from an aqueous environment.

Acknowledgements

The authors would like to acknowledge the financial support provided by a Research University grant from the University of Malaya (RU003-2021). Shahla Imteyaz acknowledges the Council of Scientific and Industrial Research (CSIR), Government of India. Volker Hessel acknowledges support from the ERC Synergy Grant "Surface-Confined fast modulated Plasma

for process and Energy intensification" (SCOPE), from the European Commission, with Grant No. 810182; to scope and benchmark wastewater processing technology for use of plasma-fixed carbon nanodots on removal of organic pollutants, under current investigation.

Conflict of interest

The authors declare no potential conflict of interest regarding the publication of this work.

References

1. R. K. Pradeev, K. Sadaiyandi, A. Kennedy, Photocatalytic and antibacterial studies of indium-doped ZnO nanoparticles synthesized by co-precipitation technique, J Mater Sci: Mater Electron. 28 (2017) 19025–19037.
2. M. Muthukumaran, P. V. Prasath, R. Kulandaivelu et al., Fabrication of nitrogen-rich graphitic carbon nitride/Cu_2O (g-C_3N_4@Cu_2O) composite and its enhanced photocatalytic activity for organic pollutants degradation, J Mater Sci: Mater Electron. 31 (2020) 2257–2268.
3. S. B. Dhanalekshmi, R. Priya, K. T. Selvi, K. A. Mangai, G. K. Weldegebrieal, S. Garg, S. Sagadevan, Microwave-assisted synthesis, characterization and photocatalytic activity of mercury vanadate nanoparticles. Inorg. Chem. Commun. 131 (2021) 108768.
4. S. Sagadevan, J. A. Lett, G. K. Weldegebrieal, W. C. Oh, S. F. Alshahateet, I. Fatimah, I. Fatimah, F. Mohammad, H. A. Al-Lohedan, S. Paiman, Enhanced gas sensing and photocatalytic activity of reduced graphene oxide loaded TiO_2 nanoparticles. Chem. Phys. Lett. 780 (2021) 138897.

5. S. Sagadevan, J. A. Lett, G. K. Weldegebrieal, S. Garg, W.-C. Oh, N. A. Hamizi, M. R. Johan, Enhanced Photocatalytic Activity of rGO-CuO Nanocomposites for the Degradation of Organic Pollutants. Catalysts 11 (2021) 1008.
6. S. Sagadevan, J. A. Lett, G. K. Weldegebrieal, S. Imteyaz, M. R. Johan, Synthesis, characterization, and photocatalytic activity of PPy/SnO_2 nanocomposite. Chemical Physics Letters 783 (2021) 139051.
7. J. N. Naat, Y. A. B. Neolaka, T. Lapailaka, T. R. Rachmat Triandi, A. Sabarudin, H. Darmokoesoemo, H. S. Kusuma, Adsorption of Cu(II) and Pb(II) using silica@mercapto (hs@m) hybrid adsorbent synthesized from silica of Takari sand: Optimization of parameters and kinetics. Rasayan Journal of Chemistry 14(1) (2021) 550-560.
8. E. P. Kuncoro, T. Soedarti, T. Widyaleksono C. Putranto, H. Darmokoesoemo, N. R. Abadi, H. S. Kusuma, Characterization of a mixture of algae waste-bentonite used as adsorbent for the removal of Pb^{2+} from aqueous solution. Data in Brief 16 (2018) 908-913.
9. E. P. Kuncoro, D. R. M. Isnadina, H. Darmokoesoemo, O. R. Fauziah, H. S. Kusuma, Characterization, kinetic, and isotherm data for adsorption of Pb^{2+} from aqueous solution by adsorbent from mixture of bagasse-bentonite. Data in Brief 16 (2018) 622-629.
10. E. P. Kuncoro, D. R. M. Isnadina, H. Darmokoesoemo, F. Dzembarahmatiny, H. S. Kusuma, Characterization and isotherm data for adsorption of Cd^{2+} from aqueous solution by adsorbent from mixture of bagasse-bentonite. Data in Brief 16 (2018) 354-360.
11. R. A. Khera, M. Iqbal, A. Ahmad, S. M. Hassan, A. Nazir, A. Kausar, H. S. Kusuma, J. Niasr, N. Masood, U. Younas, R. Nawaz, M. I. Khan Kinetics and equilibrium studies of copper, zinc, and nickel ions adsorptive removal on to Archontophoenix alexandrae: conditions optimization by RSM. 201 (2020)289-300.
12. A. Subashini, P.V. Prasath, S. Sagadevan, J. A. Lett, I. Fatimah, F. Mohammad, H.A. Al-Lohedan, S. F. Alshahateet, W. C. Oh, Enhanced photocatalytic degradation efficiency of

graphitic carbon nitride-loaded CeO_2 nanoparticles. Chemical Physics Letters 769 (2021) 138441.

13. S. Munusamy, K. Sivaranjan, P. Sabhapathy, P. S. Ramesh, V. Narayanan, F. Mohammad, S. Sagadevan, Electrochemical and photocatalytic studies of Ta_3N_5-TaON-PEDOT-PANI nanohybrids. Chemical Physics Letters 780 (2021) 138947.
14. H. Darmokoesoemo, F. R. Setianingsih, T. W. L. C. Putranto, H. S. Kusuma, horn snail (telescopium sp) and mud crab (scylla sp) shells powder as low-cost adsorbents for removal of cu^{2+} from synthetic wastewater. RASĀYAN Journal of Chemistry 9 (2016) 550-555.
15. H. Darmokoesoemo, Magdhalena, T. W. L. C. Putranto, H. S. Kusuma1, Telescope snail (telescopium sp) and mangrove crab (scylla sp) as adsorbent for the removal of pb^{2+} from aqueous solutions, RASĀYAN Journal of Chemistry 9 (2016) 680-685.
16. J. E. Efome, D. Rana, T. Matsuura, C. Q. Lan, Experiment and modeling for flux and permeate concentration of heavy metal ion in adsorptive membrane filtration using a metal-organic framework incorporated nanofibrous membrane. Chemical Engineering Journal 352 (2018) 737–744.
17. J. E. Efome, D. Rana, T. Matsuura, C. Q. Lan, Effects of operating parameters and coexisting ions on the efficiency of heavy metal ions removal by nano-fibrous metal-organic framework membrane filtration process. Science of the Total Environment 674 (2019) 355–362.
18. J. E. Efome, D. Rana, T. Matsuura, C. Q. Lan, Insight Studies on Metal-Organic Framework Nanofibrous Membrane Adsorption and Activation for Heavy Metal Ions Removal from Aqueous Solution. ACS Appl. Mater. Interfaces 10 (2018) 18619−18629.
19. J. E. Efome, D. Rana, T. Matsuura, C. Q. Lan, Metal–organic frameworks supported on nanofibers to remove heavy metals. J. Mater. Chem. A 6 (2018) 4550-4555.

20. N. A. A. Qasem, R. H. Mohammed, D. U. Lawal, Removal of heavy metal ions from wastewater: a comprehensive and critical review. npj Clean Water 4 (2021) 36.
21. R. K. Pradeev, K. Sadaiyandi, A. Kennedy, Influence of Mg Doping on ZnO Nanoparticles for Enhanced Photocatalytic Evaluation and Antibacterial Analysis. Nanoscale Res Lett 13(2018) 229.
22. D. Hariharan, A. J. Christy, S. Pitchaiya, Green hydrothermal synthesis of gold and palladium doped titanium dioxide nanoparticles for multifunctional performance. J Mater Sci: Mater Electron 30 (2019) 12812–12819.
23. M. Muthukumaran, G. Gnanamoorthy, P. V. Prasath, M. Abinaya, G. Dhinagaran, S. Sagadevan, F. Mohammad, W. C. Oh, K Venkatachalam, Enhanced photocatalytic activity of Cuprous Oxide nanoparticles for malachite green degradation under the visible light radiation. Mater. Res. Express 7 (2020) 015038.
24. W. Li, J. Liu, D. Zhao Mesoporous materials for energy conversion and storage devices. Nature Reviews Materials 1 (2016) 16023.
25. E. Duraisamy, H. T. Das, A. S. Sharma, P. Elumalai, Supercapacitor and photocatalytic performances of hydrothermally-derived Co_3O_4/CoO@carbon nanocomposite. New Journal of Chemistry 42 (2018) 6114-6124.
26. S. M. Pourmortazavi, M. R. Nasrabadi, M. S. Karimi, S. Mirsadeghi, Evaluation of photocatalytic and supercapacitor potential of nickel tungstate nanoparticles synthesized by electrochemical method. New Journal of Chemistry 42 (2018) 19934-19944.
27. R. Edla, N. Patel, Z. El Koura, R. Fernandes, N. Bazzanella, A. Miotello, Pulsed laser deposition of Co_3O_4 nanocatalysts for dye degradation and CO oxidation. Applied Surface Science 302 (2014) 105-108.

28. Y. Zheng, W. Wang, D. Jiang, L. Zhang, X. Li, Z. Wang , Ultrathin mesoporous Co_3O_4 nanosheets with excellent photo-/thermo-catalytic activity. Journal of Materials Chemistry A 4 (2016) 105-112.
29. A. Sudhaik, P. Raizada, P. Shandilya, P. Singh, Magnetically recoverable graphitic carbon nitride and $NiFe_2O_4$ based magnetic photocatalyst for degradation of oxytetracycline antibiotic in simulated wastewater under solar light. J. Environ. Chem. Eng. 6 (4) (2018) 3874–3883.
30. K. Kabra, R. Chaudhary, R. L. Sawhney, Treatment of hazardous organic and inorganic compounds through aqueous phase photocatalysis: a review. Ind. Eng. Chem. Res. 43 (24) (2004) 7683–7696.
31. P. Raizada, A. Sudhaik, S. Patial, V. Hasija, A. A. P. Khan, P. Singh, S. Gautam, M. Kaur, V. -H. Nguyen, Engineering nanostructures of CuO-based photocatalysts for water treatment: Current progress and future challenges. Arabian Journal of Chemistry 13 (11) (2020) 8424-8457.
32. A. Sharma, B. K. Lee, Structure and activity of TiO_2/FeO co-doped carbon spheres for adsorptive-photocatalytic performance of complete toluene removal from aquatic environment. Appl. Catal. A: Gen. 523 (2016) 272–282.
33. M. Mohsin, I. A. Bhatti, A. Ashar, M. W. Khan, M. U. Farooq, H. Khan, M. T. Hussain, S. Loomba, M. Mohiuddin, A. Zavabeti, Iron-doped zinc oxide for photocatalyzed degradation of humic acid from municipal wastewater. Appl. Mater. Today 23 (2021) 101047.
34. Y. Li, X. Y. Yang, Y. Feng, Z. Y. Yuan, B. L. Su, One dimensional metal oxide nanotube, nanowires, nanoribbons, and nanorods: synthesis, characterizations, properties and applications. Crit. Rev. Solid. State. Mater. Sci. 37 (1) (2012) 1–74.

35. T. Ravishankar, M. d. O. Vaz, S. Teixeira, The effects of surfactant in the sol–gel synthesis of CuO/TiO_2 nanocomposites on its photocatalytic activities under UV-visible and visible light illuminations. New Journal of Chemistry 44 (2020) 1888-1904.
36. Z. Xu, J. Xu, J. Ni, F. Hu, J. Xu, Visible light catalytic reduction of Cr (VI) by palygorskite modified with CuO in the presence of tartaric acid. Environmental Engineering Science 36 (2019) 491-498.
37. Z. Xu, Y. Yu, D. Fang, J. Liang, L. Zhou, Simulated solarlight catalytic reduction of Cr (VI) on microwave–ultrasonication synthesized flower-like CuO in the presence of tartaric acid. Materials Chemistry and Physics 171 (2016) 386-393.
38. A. Samad, M. Furukawa, H. Katsumata, T. Suzuki, S. Kaneco, Photocatalytic oxidation and simultaneous removal of arsenite with CuO/ZnO photocatalyst. Journal of Photochemistry and Photobiology A: Chemistry 325 (2016) 97-103.
39. B. Nanda, A. C. Pradhan, K. M. Parida, Fabrication of mesoporous CuO/ZrO_2-MCM-41 nanocomposites for photocatalytic reduction of Cr(VI). Chemical Engineering Journal 316 (2017) 1122-1135.
40. T. Sun, Z. Zhao, Z. Liang, J. Liu, W. Shi, F. Cui, Efficient As(III) removal by magnetic $CuO\text{-}Fe_3O_4$ nanoparticles through photo-oxidation and adsorption under light irradiation. Journal of Colloid and Interface Science 495 (2017) 168-177.
41. J. Kondabey, M. H. Ghorbani, H. Aghaie, R. Fazaeli, Study of the adsorption and photocatalytic properties of copper oxide with different morphologies in removal of Cr(III) ion from aqueous media. Water Science and Technology 80 (2019) 827-835.
42. S. C. Lee, Y. Jeong, Y. J. Kim, H. Kim, H. U. Lee, Y. -C. Lee, S. M. Lee, H. J. Kim, H. -R An, M. G. Ha, G. -W. Lee, Y. -S. Lee, G. Lee, Hierarchically three-dimensional (3D) nanotubular sea urchin-shaped iron oxide and its application in heavy metal removal and

solar-induced photocatalytic degradation. Journal of Hazardous Materials 354 (2018) 283-292.

43. F. A. Harraz, O. E. A. -Salam, A. A. Mostafa, R. M. Mohamed, M. Hanafy, Rapid synthesis of titania–silica nanoparticles photocatalyst by a modified sol–gel method for cyanide degradation and heavy metals removal. Journal of Alloys and Compounds 551 (2013) 1-7.
44. Q. Wang, N. Zhu, E. Liu, C. Zhang, J. C. Crittenden, Y. Zhang, Y. Cong, Fabrication of visible-light active Fe_2O_3-GQDs/NF-TiO_2 composite film with highly enhanced photoelectrocatalytic performance. Applied Catalysis B: Environmental 205 (2017) 347-356.
45. Q. Wang, Q. Gao, H. Wu, Y. Fan, D. Lin, Q. He, Y. Zhang, Y. Cong, In situ construction of semimetal Bi modified BiOI-Bi_2O_3 film with highly enhanced photoelectrocatalytic performance. Separation and Purification Technology 226 (2019) 232-240.
46. Y. Zhang, Q. Wang, J. Lu, Q. Wang, Y. Cong, Synergistic photoelectrochemical reduction of Cr(VI) and oxidation of organic pollutants by g-C_3N_4/TiO_2-NTs electrodes. Chemosphere 162 (2016) 55-63.
47. L. Cheng, S. Liu, G. Hea, Y. Hu, The simultaneous removal of heavy metals and organic contaminants over a Bi_2WO_6/mesoporous TiO_2 nanotube composite photocatalyst. RSC Adv 10 (2020) 21228-21237.
48. G. K. Weldegebrieal, Synthesis method, antibacterial and photocatalytic activity of ZnO nanoparticles for azo dyes in wastewater treatment: a review. Inorg Chem Commun 120 (2020) 108140.
49. F. Azeez, E. Al-Hetlani, M. Arafa, Y. Abdelmonem, A. A. Nazeer, M. O. Amin, M. Madkour, The effect of surface charge on photocatalytic degradation of methylene blue dye using chargeable titania nanoparticles. Scientific Reports 8 (2018) 7104.

50. E. N. Bakatula, D. Richard, C. M. Neculita, G. J. Zagury, Determination of point of zero charge of natural organic materials. Environmental Science and Pollution Research 25 (2018) 7823-7833.
51. M. Chauhan, N. Kaur, P. Bansal, R. Kumar, S. Srinivasan, G. R. Chaudhary, Proficient Photocatalytic and Sonocatalytic Degradation of Organic Pollutants Using CuO Nanoparticles. Journal of Nanomaterials 2020 (2020) 6123178.
52. F. Mahdizadeh, S. Aber, Treatment of textile wastewater under visible LED lamps using CuO/ZnO nanoparticles immobilized on scoria rocks. RSC Advances 5 (2015) 75474-75482.
53. W. -f. Tan, S. -j. Lu, F. Liu, X. -h. Feng, J. -z. He, L. K. Koopal, Determination Of The Point-Of-Zero Charge Of Manganese Oxides With Different Methods Including An Improved Salt Titration Method. Soil Science 173 (2008) 277-286.
54. A. L. K. Venkata, S. P. Anthony, M. S. Muthuraman, Synthesis of Solanum nigrum mediated copper oxide nanoparticles and their photocatalytic dye degradation studies. Materials Research Express 6 (2019) 125402.
55. R. Banu, N. Salvi, C. Ameta, R. Ameta, P. B. Punjabi, Visible light driven photocatalytic degradation of brilliant green dye using graphene oxide/copper oxide binary composite. 58B (02) (2019) 157-166.
56. M. P. Rao, J. J. Wu, A. Syed, F. Ameen, S. Anandan, Synthesis of Dandelion—like CuO microspheres for photocatalytic degradation of reactive black-5. Materials Research Express 5 (2018) 015053.
57. S. Norzaee, B. Djahed, R. Khaksefidi, F. K. Mostafapour, Photocatalytic degradation of aniline in water using CuO nanoparticles. Journal of Water Supply: Research and Technology—Aqua 66 (2017) 178-185.

58. Y. -B. Feng, L. Hong, A. -L. Liu, W. -D. Chen, G. -W. Li, W. Chen, X. -H. Xia, High-efficiency catalytic degradation of phenol based on the peroxidase-like activity of cupric oxide nanoparticles. International Journal of Environmental Science and Technology 12 (2015) 653-660.
59. E. A. Zeid, I. Ibrahem, W. A. Mohamed, A. M. Ali, Study the influence of silver and cobalt on the photocatalytic activity of copper oxide nanoparticles for the degradation of methyl orange and real wastewater dyes. Materials Research Express 7 (2020) 026201.
60. P. Nuengmatcha, P. Porrawatkul, S. Chanthai, P. Sricharoen, N. Limchoowong, Enhanced photocatalytic degradation of methylene blue using Fe_2O_3/graphene/CuO nanocomposites under visible light. Journal of Environmental Chemical Engineering 7 (2019) 103438.
61. N. Kumaresan, M. M. A. Sinthiya, K. Ramamurthi, R. R. Babu, K. Sethuraman, Visible light driven photocatalytic activity of ZnO/CuO nanocomposites coupled with rGO heterostructures synthesized by solid-state method for RhB dye degradation. Arabian Journal of Chemistry 13 (2020) 3910-3928.
62. P. Amirian, E. Bazrafshan, A. Payandeh, Textile Wastewater Treatment Using Photonanocatalytic Process (UV/CuO Nanoparticles): Optimization of Experiments by Response Surface Methodology. Health Scope 7 (2018).
63. D. Malwal, P. Gopinath, Enhanced photocatalytic activity of hierarchical three dimensional metal oxide@ CuO nanostructures towards the degradation of Congo red dye under solar radiation. Catalysis Science & Technology 6 (2016) 4458-4472.
64. R. Nayak, F. A. Ali, D. K. Mishra, D. Ray, V. Aswal, S. K. Sahoo, B. Nanda, Fabrication of CuO nanoparticle: an efficient catalyst utilized for sensing and degradation of pheno. Journal of Materials Research and Technology 9 (2020) 11045-11059.
65. A. N. -Ejhieh, M. Amiri, CuO supported Clinoptilolite towards solar photocatalytic degradation of p-aminophenol. Powder Technology 235 (2013) 279-288.

66. M. Rafique, F. Shafiq, S. S. A. Gillani, M. Shakil, M. B. Tahir, I. Sadaf, Eco-friendly green and biosynthesis of copper oxide nanoparticles using Citrofortunella microcarpa leaves extract for efficient photocatalytic degradation of Rhodamin B dye form textile wastewater. Optik 208 (2020) 164053.
67. S. Senobari, A. N. Ejhieh, A comprehensive study on the photocatalytic activity of coupled copper oxide-cadmium sulfide nanoparticles. Spectrochimica Acta Part A: Molecular and Biomolecular Spectroscopy 196 (2018) 334-343.
68. A. S. -Mohammadia, Z. Ghorbanianb, G. Asgaria, A. Dargahic, Photocatalytic degradation of metronidazole (MNZ) antibiotic in aqueous media using copper oxide nanoparticles activated by H_2O_2/UV process: biodegradability and kinetics studies. Desalination and Water Treatment 193 (2020) 369-380.
69. A. Iqbal, A. U. Haq, G. A. C. -Calle, S. A. R. Naqvi, P. Westerhoff, S. G. -Segura, Green Synthesis of Flower-Shaped Copper Oxide and Nickel Oxide Nanoparticles via Capparis decidua Leaf Extract for Synergic Adsorption-Photocatalytic Degradation of Pesticides. Catalysts 11 (2021) 806.
70. A. Chakraborty, D. A. Islam, H. Acharya, Facile synthesis of CuO nanoparticles deposited zeolitic imidazolate frameworks (ZIF-8) for efficient photocatalytic dye degradation. Journal of Solid State Chemistry 269 (2019) 566-574.
71. K. Pakzad, H. Alinezhad, M. Nasrollahzadeh, Green synthesis of Ni@Fe_3O_4 and CuO nanoparticles using Euphorbia maculata extract as photocatalysts for the degradation of organic pollutants under UV-irradiation. Ceramics International 45 (2019) 17173-17182.
72. V. Kumari, S. Yadav, J. Jindal, S. Sharma, K. Kumari, N. Kumar, Synthesis and characterization of heterogeneous ZnO/CuO hierarchical nanostructures for photocatalytic degradation of organic pollutant. Advanced Powder Technology 31 (2020) 2658-2668.

73. Z. Behzadifard, Z. Shariatinia, M. Jourshabani, Novel visible light driven CuO/$SmFeO_3$ nanocomposite photocatalysts with enhanced photocatalytic activities for degradation of organic pollutants. Journal of Molecular Liquids 262 (2018) 533-548.
74. F. Poorsajadi, M. H. Sayadi, M. Hajiani, M. R. Rezaei, Synthesis of CuO/Bi_2O_3 nanocomposite for efficient and recycling photodegradation of methylene blue dye. International Journal of Environmental Analytical Chemistry (2020) 1-14.
75. M. Kositzi, I. Poulios, K. Samara, E. Tsatsaroni, E. Darakas, Photocatalytic oxidation of cibacron yellow LS-R. Journal of hazardous materials 146 (2007) 680-685.
76. C. Chen, J. Liu, P. Liu, B. Yu, Investigation of photocatalytic degradation of methyl orange by using nano-sized ZnO catalysts. Advances in Chemical Engineering and Science 1 (2011) 9.
77. Y. -H. Chiu, T. -F. M. Chang, C. -Y. Chen, M. Sone, Y. -J. Hsu, Mechanistic Insights into Photodegradation of Organic Dyes Using Heterostructure Photocatalysts. Catalysts 9 (2019) 430.
78. P. Nuengmatcha, P. Porrawatkul, S. Chanthai, P. Sricharoen, N. Limchoowong, Enhanced photocatalytic degradation of methylene blue using Fe_2O_3/graphene/CuO nanocomposites under visible light. Journal of Environmental Chemical Engineering 7 (2019) 103438.
79. M. Rafique, M. B. Tahir, M. Irshad, G. Nabi, S. S. A. Gillani, T. Iqbal, M. Mubeen, Novel Citrus aurantifolia leaves based biosynthesis of copper oxide nanoparticles for environmental and wastewater purification as an efficient photocatalyst and antibacterial agent. Optik 219 (2020) 165138.
80. M. Rafique, F. Shafiq, S. S. Ali Gillani, M. Shakil, M. B. Tahir, I. Sadaf, Eco-friendly green and biosynthesis of copper oxide nanoparticles using Citrofortunella microcarpa leaves extract for efficient photocatalytic degradation of Rhodamin B dye form textile wastewater. Optik 208 (2020) 164053.

81. A. G. A. -Mendoza, A. I. -Molina, D. V. -Hernández, C. A. C. -Sánchez, E. R. -Castellón, J. C. T. -Córdova, Photodegradation of methylene blue and methyl orange with CuO supported on ZnO photocatalysts: The effect of copper loading and reaction temperature. Materials Science in Semiconductor Processing 119 (2020) 105257.
82. S. Sohrabi, F. Akhlaghian, Surface investigation and catalytic activity of iron-modified TiO_2. Journal of Nanostructure in Chemistry 6 (2016) 93-102.
83. M. S. Nasrollahzadeh, M. Hadavifar, S. S. Ghasemi, M. A. Chamjangali, Synthesis of ZnO nanostructure using activated carbon for photocatalytic degradation of methyl orange from aqueous solutions. Applied Water Science 8 (2018) 104.
84. Kinetic Study on Photocatalytic Degradation of 4BS Azo Dye Over TiO_2 in Slurry. Environmental Engineering Science 23 (2006) 1000-1008.
85. B. Bajorowicz, M. Kobylański, A. Malankowska, P. Mazierski, J. Nadolna, A. Pieczyńska, A. Z. -Medynska, Application of metal oxide-based photocatalysis. (2018).
86. N. Khoshnamvand, F. Kord Mostafapour, A. Mohammadi, M. Faraji, Response surface methodology (RSM) modeling to improve removal of ciprofloxacin from aqueous solutions in photocatalytic process using copper oxide nanoparticles (CuO/UV). AMB Express 8 (2018) 48.
87. A. U. Khan, A. U. Khan, B. Li, M. H. Mahnashi, B. A. Alyami, Y. S. Alqahtani, K. Tahir, S. Khan, S. Nazir, A facile fabrication of silver/copper oxide nanocomposite: An innovative entry in photocatalytic and biomedical materials. Photodiagnosis and Photodynamic Therapy 31 (2020) 101814.
88. E. Mousset, N. Oturan, M. A. Oturan, An unprecedented route of OH radical reactivity evidenced by an electrocatalytical process: Ipso-substitution with perhalogenocarbon compounds. Applied Catalysis B: Environmental 226 (2018) 135-146.

89. M. Pirilä, M. Saouabe, S. Ojala, B. Rathnayake, F. Drault, A. Valtanen, M. Huuhtanen, R. Brahmi, R. L. Keiski, Photocatalytic degradation of organic pollutants in wastewater. Topics in Catalysis 58 (2015) 1085-1099.
90. S. G. -Rodríguez, E. Rodríguez, D. N. Singh, J. R. -Chueca, Assessment of sulfate radical-based advanced oxidation processes for water and wastewater treatment: a review. Water 10 (2018) 1828.
91. N. Mukwevho, E. Fosso-Kankeu, F. Waanders, N. Kumar, S. S. Ray, X. Y. Mbianda, Photocatalytic activity of $Gd_2O_2CO_3$ ZnO CuO nanocomposite used for the degradation of phenanthrene. SN Applied Sciences 1 (2019) 1-11.
92. A. Sharma, R. K. Dutta, Studies on the drastic improvement of photocatalytic degradation of acid orange-74 dye by TPPO capped CuO nanoparticles in tandem with suitable electron capturing agents. RSC Advances 5 (2015) 43815-43823.
93. A. H. Abdullah, W. -Y. Wong, M. I. Yaziz, Decolorization of reactive orange 16 dye by copper oxide syste. Sains Malaysiana 39 (2010) 587-591.
94. S. Hong, Y. Yu, Z. Yi, H. Zhu, W. Wu, P. Ma, Highly efficient and recyclable g-C_3N_4/CuO hybrid nanocomposite towards enhanced visible-light photocatalytic performance. Nano, 11 (2016) 1650121.
95. E. M. Saggioro, A. S. Oliveira, J.C. Moreira, Heterogeneous photocatalysis remediation of wastewater polluted by indigoid dyes. Text Wastewater Treat (2016).
96. S. M. M. Kabir, J. Koh, Dyeing Chemicals, in: Chemistry and Technology of Natural and Synthetic Dyes and Pigments. IntechOpen 2018.
97. S. Senobari, A. N. -Ejhieh, A comprehensive study on the enhanced photocatalytic activity of CuO-NiO nanoparticles: Designing the experiments. Journal of Molecular Liquids 261 (2018) 208-217.

98. Y. Su, S. Li, G. Jiang, Z. Zheng, C. Wang, S. Zhao, D. Cui, Y. Liu, B. Zhang, Z. Zhang, Synergic removal of tetracycline using hydrophilic three-dimensional nitrogen-doped porous carbon embedded with copper oxide nanoparticles by coupling adsorption and photocatalytic oxidation processes. Journal of Colloid and Interface Science 581 (2021) 350-361.

99. S. Shekoohiyan, A. Rahmania, M. Chamack, G. Moussavi, O. Rahmanian, V. Alipour, S. Giannakis, A novel CuO/Fe_2O_3/ZnO composite for visible-light assisted photocatalytic oxidation of Bisphenol A: Kinetics, degradation pathways, and toxicity elimination. Separation and Purification Technology 242 (2020) 116821.

100. M. Wang, C. Jin, J. Kang, J. Liu, Y. Tang, Z. Li, S. Li, CuO/g-C_3N_4 2D/2D heterojunction photocatalysts as efficient peroxymonosulfate activators under visible light for oxytetracycline degradation: Characterization, efficiency and mechanism. Chemical Engineering Journal 416 (2021) 128118.

101. M. Nazim, A. A. P. Khan, A. M. Asiri, J. H. Kim, Exploring Rapid Photocatalytic Degradation of Organic Pollutants with Porous CuO Nanosheets: Synthesis, Dye Removal, and Kinetic Studies at Room Temperature. ACS Omega 6 (2021) 2601-2612.

102. Z. A. Mahar, G. Q. Shar, A. Balouch, A. H. Pato, A. R. Shaikh, Effective and viable photocatalytic degradation of rhodamine B dye in aqueous media using CuO/PVA nanocomposites. New J. Chem. 45 (2021) 16500-16510.

103. G. Manjari, S. Saran, T. Arun, A. V. B. Rao, S. P. Devipriya, Catalytic and recyclability properties of phytogenic copper oxide nanoparticles derived from Aglaia elaeagnoidea flower extract. Journal of Saudi Chemical Society 21 (2017) 610-618.

104. I. Khan, I. Khan, M. Usman, M. Imran, K. Saeed, Nanoclay-mediated photocatalytic activity enhancement of copper oxide nanoparticles for enhanced methyl orange

photodegradation. Journal of Materials Science: Materials in Electronics 31 (2020) 8971-8985.

105. Y. Haldorai, J. -J. Shim, Multifunctional Chitosan-Copper Oxide Hybrid Material: Photocatalytic and Antibacterial Activities. International Journal of Photoenergy 2013 (2013) 245646.

106. F. Soori, A. N. -Ejhieh, Synergistic effects of copper oxide-zeolite nanoparticles composite on photocatalytic degradation of 2,6-dimethylphenol aqueous solution. Journal of Molecular Liquids 255 (2018) 250-256.

107. N. F. Khairol, N. Sapawe, M. Danish, Excellent Performance Integrated Both Adsorption and Photocatalytic Reaction Toward Degradation of Congo Red by CuO/Eggshell. Materials Today: Proceedings 19 (2019) 1340-1345

108. M. A. Barakat, New trends in removing heavy metals from industrial wastewater. Arabian Journal of Chemistry 4 (2011) 361-377.

109. Z. Zhao, H. An, J. Lin, M. Feng, V. Murugadoss, T. Ding, H. Liu, Q. Shao, X. Mai, N. Wang, H. Gu, S. Angaiah, Z. Guo, Progress on the Photocatalytic Reduction Removal of Chromium Contamination. The Chemical Record 19 (2019) 873-882.

110. M. M. Rahman, M. M. Alam, A. M. Asiri, Fabrication of selective and sensitive chemical sensor probe based on ternary nano-formulated $CuO/MnO_2/Gd_2O_3$ spikes by hydrothermal approach. Sci Rep 10 (2020) 20248.

111. X. Tian, L. Liu, Y. Li, C. Yang, Z. Zhou, Y. Nie, Y. Wang, Nonenzymatic electrochemical sensor based on $CuO\text{-}TiO_2$ for sensitive and selective detection of methyl parathion pesticide in ground water. Sensors and Actuators B: Chemical 256 (2018) 135-142.

112. M. M. Rahman, A. M. Asiri, Development of selective and sensitive bicarbonate chemical sensor based on wet-chemically prepared CuO-ZnO nanorods. Sensors and Actuators B: Chemical 214 (2015) 82-91.

113. M. M. Rahman, M. M. Alam, M. M. Hussain, A. M. Asiri, M. E. M. Zayed, Hydrothermally prepared Ag_2O/CuO nanomaterial for an efficient chemical sensor development for environmental remediation. Environmental Nanotechnology, Monitoring & Management 10 (2018) 1-9.

114. M.A. Bajiri, A. Hezam, K. Namratha, R. Viswanath, Q. Drmosh, H.B. Naik, K. Byrappa, CuO/ZnO/g-C3N4 heterostructures as efficient visible light-driven photocatalysts, Journal of Environmental Chemical Engineering, 7 (2019) 103412.

115. D. Chen, A. K. Ray, Removal of toxic metal ions from wastewater by semiconductor photocatalysis. Chemical Engineering Science 56 (2001) 1561-1570.

116. A. Mohagheghian, N. B. -Givi, K. Godini, R. Dewil, M. S. -Siboni, Photocatalytic reduction of Cr(VI) from aqueous solution by visible light/CuO-Kaolin: Optimization and modeling of key parameters using central composite design (CCD). Separation Science and Technology 56 (2021) 1253-1271.